Research Article Vol. 31, No. 1 / 2 Jan 2023 / Optics Express 745
Optics EXPRESS

Realization of CW single-frequency tunable Ti:sapphire laser with immunity to the noise of the pump source

JIAQI SONG,[1] JILIANG QIN,[1,2] PIXIAN JIN,[1,2] YANAN CHEN,[1] JING SU,[1,2] AND HUADONG LU[1,2,*]

[1]State Key Laboratory of Quantum Optics and Quantum Optics Devices, Institute of Opto-Electronics, Shanxi University, Taiyuan, Shanxi 030006, China
[2]Collaborative Innovation Center of Extreme Optics, Shanxi University, Taiyuan, Shanxi 030006, China
*luhuadong@sxu.edu.cn

Abstract: All-solid-state continuous-wave (CW) single-frequency tunable Ti:sapphire (Ti:S) laser is an important source in quantum optics and atomic physics. However, intracavity etalon (IE) locking is easily influenced by the intensity noise of the pump source in the low frequency band. In order to address this issue, a differential detector with dual-photodiodes (PDs) is designed and employed in the experiment. Both PDs are used to detect the lights of the pump source and the built Ti:S laser, respectively. As a result, the influence of the intensity noise of the pump source on the stability of the IE locking is successfully eliminated and the IE is stably locked to the oscillating longitudinal-mode of the laser. On this basis, a stable CW single-frequency tunable Ti:S laser is realized. The presented method is beneficial to attain a stable single-frequency tunable laser with immunity to the intensity noise of the pump source.

1. Introduction

All-solid-state continuous-wave (CW) single-frequency tunable Ti:sapphire (Ti:S) lasers have been widely applied in many cutting-edge scientific research fields including high-sensitive laser spectroscopy [1], quantum information [2], high-precision measurement [3] and so on, owing to their intrinsic advantages of broad output spectrum of 650-1050 nm, good beam quality, high output power [4] and compact structure [5]. Especially in the field of atomic physics [6], the Ti:S lasers with broad wavelength range cover multiple atom absorption lines. For example, the wavelengths of 780 nm and 795 nm correspond to the D_2 and D_1 lines of Rubidium (Rb) atoms [7], respectively, and the wavelengths of 852 nm and 894 nm laser cover the D_2 and D_1 lines of Cesium (Cs) atoms [8]. In order to accurately match the atom absorption lines, it is necessary to realize the continuous frequency-tuning of the Ti:S laser with the mode-hopping-free. As early as 1997, a novel method for achieving continuous frequency-tuning of a CW single-frequency laser was developed, which was implemented by inserting a nonlinear crystal into the resonator. Because the nonlinear losses of non-lasing modes are twice that of lasing mode, the axial mode-hopping was suppressed and single-frequency operation of the laser in the process of frequency-tuning was realized [9]. In 2014, our group for the first time applied this method to the Ti:S laser by inserting a nonlinear BIBO crystal into the resonator, and the continuous frequency-tuning up to 48 GHz with the mode-hopping-free was attained [10]. Based on nonlinear loss, our group also realized an ultra-broad continuously tunable single-frequency 532 nm laser with the continuous tuning range over 222 GHz in 2018 [11]. Recently, Yang et al. [12,13] successfully extend this method to the investigation of the single-frequency Raman lasers and obtained good results. However, restricted by the phase matching bandwidth of the nonlinear crystal, the continuous frequency-tuning can only be realized in a specific frequency range. Another popular way to accomplish the continuous frequency-tuning of a laser is to employ an intracavity etalon (IE) as

#479558 https://doi.org/10.1364/OE.479558
Journal © 2023 Received 28 Oct 2022; revised 5 Dec 2022; accepted 12 Dec 2022; published 23 Dec 2022

Optics EXPRESS

the mode selecting element. After the transmission peak of the IE is locked onto the oscillating longitudinal-mode of the laser, the transmission peak of the IE is shifted with the sliding of the laser oscillating longitudinal-mode by continuously scanning the laser cavity length, and then the continuous frequency-tuning with mode-hop-free is achieved. In 1992, Harrison et al. realized the mode selective tuning of a single-frequency laser by inserting an etalon into the cavity [14]. Nowadays, almost all commercial Ti:S lasers employ piezoelectric transducer-based (PZT-based) IE locking systems, where the frequency of the modulation signal has to correspond to the resonant frequency of the PZT, generally in the kilohertz region [15]. The introduced modulation signal increases the additional intensity noise at the corresponding frequency of the laser [16]. Although employing an electro-optic etalon can break though the frequency restriction of the modulation signal, the influenceis of the modulation signal on the intensity noise of the laser is still not dismissed [17]. In 2004, K. S. Gardner et al. presented a method by adopting a birefringent etalon (BE) as the intracavity mode selective element [18]. Based on the birefringent characteristic of the adopted etalon, they precisely locked the transmission peak of the BE to the oscillating longitudinal-mode, and obtained a stable single-frequency semiconductor laser. In 2022, our group realized a modulation-free CW single-frequency tunable Ti:S laser with the continuous frequency-tuning of 40 GHz based on an intracavity lithium niobate ($LiNbO_3$) BE [19]. Different from the traditional techniques and methods based on the modulated PZT [20], this method can extract the deviation between the laser longitudinal-mode and the resonant longitudinal-mode of the BE by detecting the change of the polarization state. Due to the diminish of the modulation signal, the influence of the modulation signal on the intensity noise of the laser was effectively eliminated.

In these tunable lasers with the IE locking systems, it is easy to find that the IE locking is easily influenced by many factors including parameters of the adopted etalon, performance of the laser, and pump source. Particularly, according to the intensity noise transfer function theory, the intensity noise of the pump source in the frequency band below 100 kHz is completely transferred to the built laser [21]. Because this frequency band happens to cover that of the modulation signal for IE locking, the large intensity noise of the pump source harmfully influences the IE locking process, and even directly induces the IE out of locking. However, this influence has not been paid attention to so far. In this paper, we firstly investigate the influence of the intensity noise of the pump source on the IE locking of a CW single-frequency laser. Then, a novel single-frequency tunable Ti:S laser with immunity to the noise of the pump source is presented, which is implemented by employing a differential detector to eliminate the influence of the intensity noise of the pump source on the IE locking.

2. Experimental setup

In order to investigate the influence of the intensity noise of the pump source on the IE locking and further achieve a single-frequency tunable Ti:S laser with immunity to the intensity noise of the pump source, a ring resonator cavity with four mirrors is firstly designed and built, which is shown in Fig. 1. The pump source is a homemade CW single-frequency 532 nm laser with a maximum radiation power of 20 W. The pump laser beam is collimated by a lens f_1 with a focal length of 200 mm and focused onto the Ti:S crystal by another lens f_2 with a focal length of 120 mm for optimal mode-matching. To ensure that the pump energy can be effectively absorbed by the Ti:S crystal, a half-wave plate is placed in front of the resonator to align the polarization of the pump laser. The designed resonator has a bow-tie-type ring configuration for the prevention of the spatial hole burning, which comprises a concave-convex mirror M_1 (R_{convex}=-100 mm; $R_{concave}$=100 mm), a plane-concave mirror M_2 ($R_{concave}$=100 mm), and two plane mirrors M_3 and M_4. The input mirror M_1 is coated with high transmission (HT) film at the wavelength of 532 nm and high reflection (HR) film at the wavelength of 740-890 nm. M_2 and M_3 are both coated with HR film at the wavelength of 740-890 nm. The output mirror M_4 is coated with the

Optics EXPRESS

transmission of 5.5% film for 740-890 nm laser. To scan the cavity length and realize continuous frequency-tuning, M_3 is glued to a PZT with a length of 25 mm. The incident angles of M_1 and M_2 are 15.8°, which well compensates the astigmatism caused by the Brewster-cut elements, including the Ti:S crystal, birefringent filters (BRF) and terbium gallium garnet (TGG) [22]. The Ti:S crystal with the size of Φ4 mm^2×20 mm is fixed in a closed copper block oven cooled by the circulation water and mounted between M_1 and M_2. The broad bandwidth optical diode (OD) consisting of a thin quartz plate and a TGG crystal surrounded by a permanent magnet can ensure unidirectional operation of the laser. For coarsely frequency-tuning in a broad frequency band, a three-plate BRF with thickness of 0.5 mm, 2 mm and 8 mm is inserted into the resonator with its Brewster incident angle. An etalon made of fused silica for suppressing the mode-hopping and implementing the finely frequency-tuning is adhered to the rotation axis of the galvanometer scanner (GC) and inserted into the resonator.

In general, for locking the transmission peak of the IE on the oscillating longitudinal-mode of the Ti:S laser, a modulation signal (S_1) generated from a function generator (FG) is loaded on the IE, and the intracavity light field is modulated, as shown in Fig. 2(a). The modulated light field is converted to the electrical signal by means of a photodetector (PD). Then the obtained signal is mixed with the demodulation signal (S_2) output from the FG. When the achieved signal after mixing goes through a low-pass filter, an error signal can be successfully obtained. The error signal is calculated by a proportional integral (PI) controller and loaded to the driver of the GC together with a direct current (DC) bias signal. By optimizing the amplitude and phase of signal S_2 and parameters of the PI controller, the IE is precisely locked to the oscillating longitudinal-mode of the laser. However, when the intensity noise of the pump source is transferred to the light field inside the resonator, the obtained signal converted from the PD will be denoted as,

$$L_1 = A[1 + \Delta(t)]sin(\omega t + \phi), \tag{1}$$

where ω is the frequency of S_1, A and ϕ are the amplitude and phase of the Ti:S laser, respectively. The term $\Delta(t)$ describes the intensity noise of the pump source. In this case, the obtained error signal after frequency mixing and filtering is expressed as,

$$D_1 = \frac{1}{2}AB[1 + \Delta(t)]cos(\phi - \psi), \tag{2}$$

where B and ψ are the amplitude and phase of S_2. From Eq. (2), it is clear that the intensity noise of the pump source can directly influences the error signal so much that the feedback system cannot be precisely controlled, and eventually causes chaos in the IE locking process.

A differential detector with dual-PDs is designed and employed in the experiment to replace the common detector, which flow chart of the IE locking process is shown in Fig. 2(b). The schematic diagram of the adopted differential detector is shown in Fig. 3. The differential detector consists of a subtractor and an amplifier, where the subtractor is composed of a pair of PDs (Model: 5971, Japan Hamamatsu). For both PDs, PD1 and PD2 are used to detect the light fields of the pump source and Ti:S laser, respectively. The amplitude fluctuation of pump coherent field corresponding to the intensity noise $\Delta(t)$ is assumed to be $\delta(\delta<1)$. If the amplitude of the pump laser is expressed as,

$$E_p = C(1 + \delta)cos(\omega_p t + \epsilon_p), \tag{3}$$

where C, ω_p, ϵ_p are initial amplitude, frequency and phase of E_p, respectively. The intensity of the pump laser is,

$$\begin{aligned} I_p = |E_p|^2 &= \frac{1}{2}C^2(1 + 2\delta + \delta^2) \\ &\approx \frac{1}{2}C^2(1 + 2\delta). \end{aligned} \tag{4}$$

Optics EXPRESS

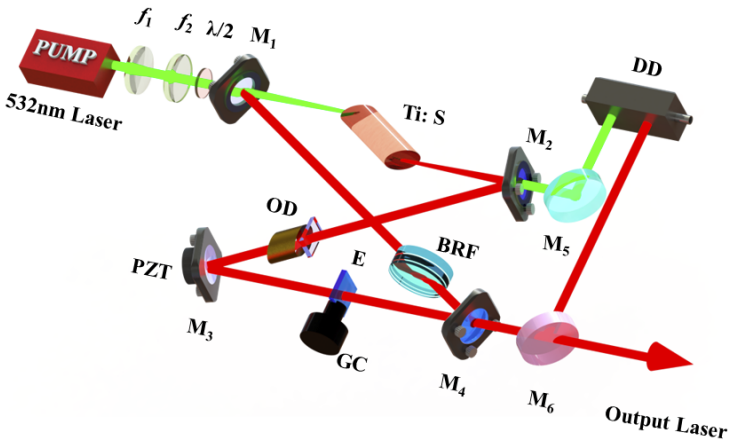

Fig. 1. Schematic diagram of the built Ti:S laser. f_1 and f_2: coupling lenses; Ti:S: titanium sapphire crystal; OD: optical diode; BRF: birefringent filters; PZT: piezoelectric transducer; E: etalon; GC: galvanometer scanner; DD: differential detector.

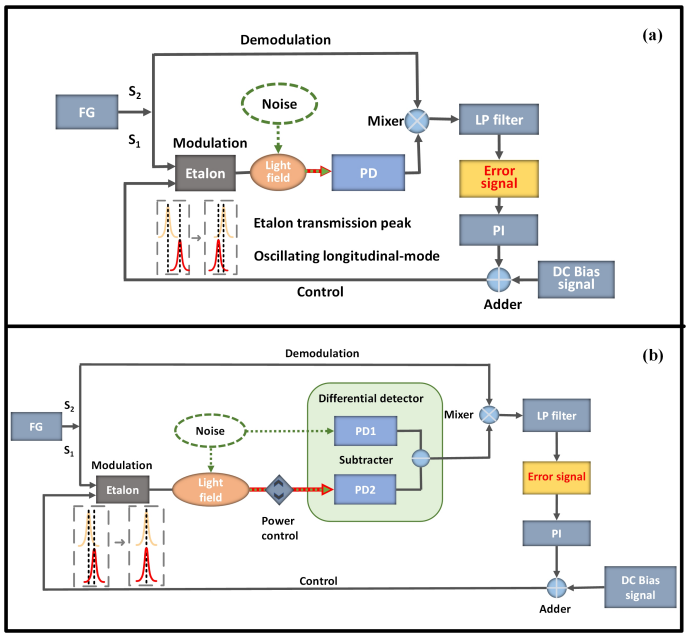

Fig. 2. Flow chart of the etalon locking process with (a) the common detector and (b) the differential detector.

Assuming the conversion factor of the light intensity between the pump source and the Ti:S laser to be κ , the Ti:S laser intensity after the modulation is expressed as,

$$\begin{aligned} I_l &= |\kappa E_p|^2[1 + sin(\omega t + \phi)] \\ &\approx \frac{1}{2}\kappa^2 C^2[1 + sin(\omega t + \phi) + 2\delta]. \end{aligned} \tag{5}$$

In the process of converting the optical signal to the electrical signal by the detector, due to the different photoelectric conversion efficiency of the PD for different wavelength lasers, the

Optics EXPRESS

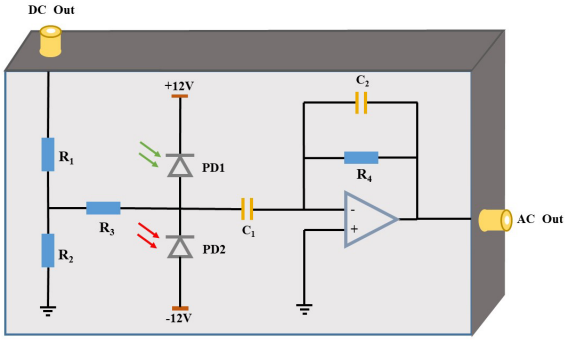

Fig. 3. Schematic diagram of the differential detector.

noises of the pump laser and Ti:S laser have to be matched by adjusting their detecting powers. Assuming that the photoelectric conversion efficiencies of PD1 and PD2 for the pump laser and Ti:S laser are α and β, respectively, in this case, only if $\beta = \frac{\alpha}{k^2}$ is satisfied, the intensity noise of the pump source can be effectively subtracted by that of the Ti:S laser, and the obtained signal is,

$$\begin{aligned} L_2 &= \beta I_l - \alpha I_p \\ &= \frac{1}{2}\alpha C^2 sin(\omega t + \phi) \\ &= F sin(\omega t + \phi), \end{aligned} \tag{6}$$

where $F = \frac{1}{2}\alpha C^2$. The obtained final error signal is expressed as,

$$D_2 = \frac{1}{2} BF cos(\phi - \psi). \tag{7}$$

Compared to Eq. (2), the error signal in Eq. (7) is no longer affected by the intensity noise of pump source. It means that using the differential detector can well eliminate the influence of the intensity noise of the pump source on the IE locking of the built Ti:S laser. In this case, the transmission peak of the IE can be stably locked to the oscillating longitudinal-mode and a stable CW single-frequency tunable Ti:S laser with immunity to the intensity noise of the pump source is realized.

3. Experimental results

In the experiment, after all of the intracavity elements are precisely aligned, the wavelength of the Ti:S laser is tuned to 824 nm, and the influence of the intensity noise of the pump source on the IE locking process is firstly investigated. The modulation signal S_1 and demodulation signal S_2 for IE locking have the same frequency of 1 kHz and their amplitudes are 100 mV and 8 V, respectively. In order to determine the noise transfer characteristics from the pump source to the built Ti:S laser, a sine wave signal with the frequency and amplitude of 1 kHz and 10 mV, respectively, is loaded on the driver of the adopted CW single-frequency 532 nm laser. The relative intensity noise (RIN) of the pump laser and 824 nm laser in the low frequency band are measured by employing a spectrum analyzer (N9010A, Agilent), respectively. The intensity noise of the pump source is directly detected from the pump laser leaked from the M_2. When PD2 is blocked and the power injected into the PD1 is about 55 mW, the RIN of the pump laser is obtained and shown as curve V_1 in Fig. 4. It is clear that there are several peaks observed in the frequency range of 0-3 kHz. Especially, the deliberately introduced signal with the frequency of 1 kHz is easily detected from the pump laser and its amplitude is about 32 dB higher than

Optics EXPRESS

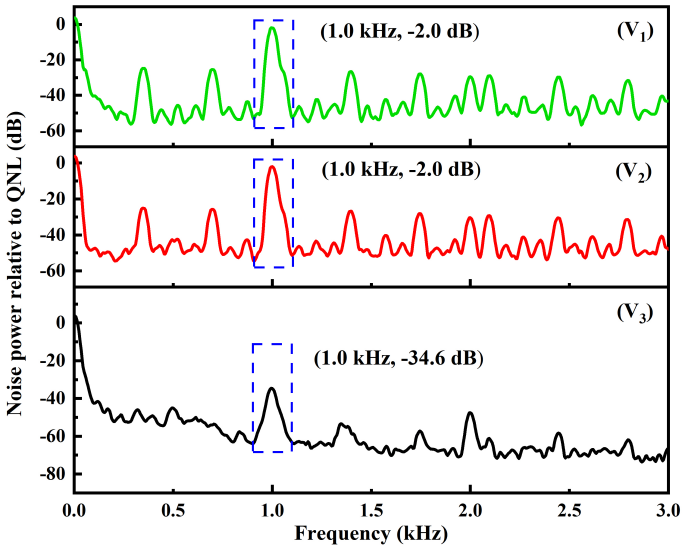

Fig. 4. Measured spectra of the intensity noise of (V_1) the pump source laser, (V_2) the Ti:S laser and (V_3) the differential signal.

the baseline. In addition to this signal and its second harmonic signals, other irregular peaks are mainly caused by the mechanical vibrations, thermal instability, power fluctuations and so on. When the PD1 and PD2 are simultaneously illuminated by the pump laser and 824 nm laser, respectively, these peaks can be reduced by precisely adjusting the incident power of the 824 nm laser with a power adjuster in front of the differential detector to about 10 mW, whose result is depicted in curve V_3. At this moment, only blocking the PD1, the RIN of the 824 nm laser is obtained as curve V_2. In this process, the injected laser powers are simultaneously recorded from the DC port of the differential detector. Comparing curves V_1 and V_2, it is seen that the intensity noise peaks of the pump source are completely transferred to the built Ti:S laser. Different from curves V_1 and V_2, the curve V_3 is generally smoother. The magnitude of the large peaks is greatly reduced, and many small peaks are submerged in the baseline, which reveals that these noise peaks in the low frequency range can be effectively reduced by employing a differential detector and precisely adjusting the incident powers of both PDs. The measured results depicted in Fig. 4 well agree to the previous theoretical predictions.

When the alternating current (AC) port of the differential detector is connected to the locking control box, the detection signal and error signal are obtained and recorded by the oscilloscope (TBS2000 SREIES, Tektronix), which are illustrated in Fig. 5. When only the PD2 is illuminated by the 824 nm laser, the detected signal shown in curve (a), it is easily seen that the large amplitude fluctuations and complex frequency signals for the detected signal are observed. Substituting data of this detected signal into the previous Eq. (2), the calculated error signal is achieved and shown in curve (b). The error signal can also be directly obtained from the servo system used in the experiment, which is shown in curve (c). Once both PD1 and PD2 are simultaneously illuminated by the lights of the pump source and 824 nm laser, respectively, a stable detected signal is achieved, which is shown in curve (d). Likewise, the error signal for this case can also be theoretical calculated according to Eq. (7) and experimental measured, which are illustrated in curves (e) and (f), respectively. From these curves, it is clear that the experimental results are in good agreement with the theoretical predictions. These results reveal that the intensity noise of the pump source is easily transferred to that of the built Ti:S laser and further influences the stability of the IE locking. Moreover, this influence can be effectively eliminated by employing

Optics EXPRESS

a differential detector and a stable CW single-frequency tunable Ti:S laser immunity to the intensity noise of the pump source is attained.

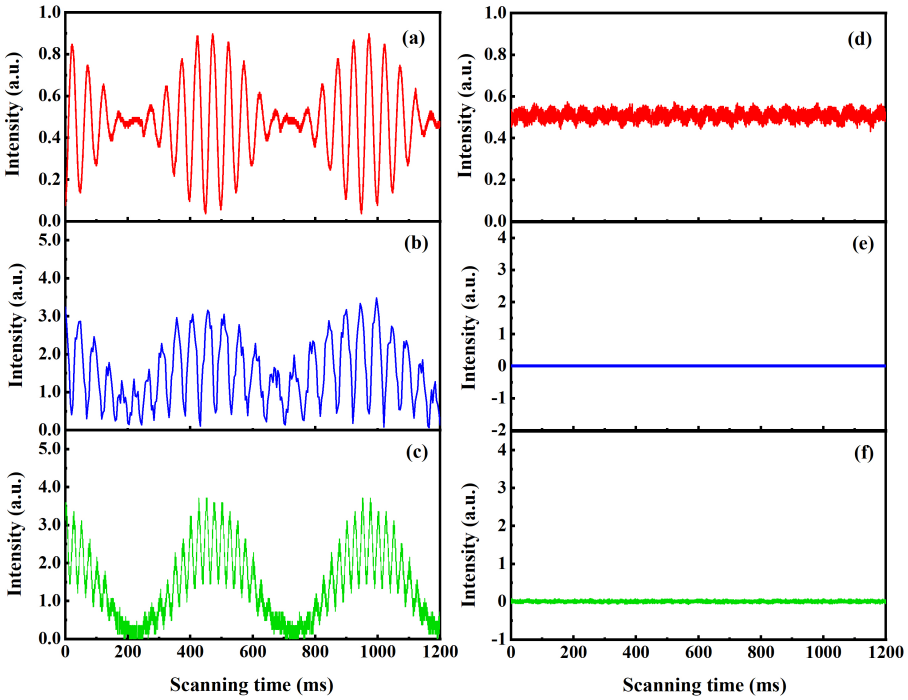

Fig. 5. (a) The detection signal measured by PD2. (b) Theoretical calculation of error signal with the pump noise. (c) The error signal measured by PD2. (d) The detection signal measured by difference detector. (e) Theoretical calculation of error signal without the pump noise. (f) The error signal measured by the difference detector.

Then, the power stability of the built Ti:S laser is compared before and after replacing the common detector with the differential detector. When the common detector is adopted, the IE could not be locked due to the large intensity noise in the low frequency band transferred from the pump source, and the Ti:S laser works with the multi-mode and mode-hopping operations. The peak-to-peak power fluctuation of free-running 824 nm laser measured by a power meter (LabMax-Top, Coherent) is ±7.2% in 3 hours. After achieving the immunity to the intensity noise of the pump source by employing the differential detector, the peak-to-peak power fluctuation of the Ti:S laser is less than ± 0.84% during 3 hours which is shown in Fig. 6. It is clear that the performance of the laser is obviously improved after adopting the differential detection to achieve the IE locking. By employing a confocal F-P interferometer with FSR of 750 MHz (F-P-100, Yuguang Co., Ltd.), the longitudinal-mode structure of the Ti:S laser is monitored and the result is depicted in inset of Fig. 6, which shows that the laser can operate with the stable single-longitudinal-mode (SLM). The transverse-mode characteristic of the obtained Ti:S laser is also measured by a M^2 beam quality analyzer (M2SETVIS, Thorlabs), and the results are depicted in Fig. 7. The measured values of M_X^2 and M_Y^2 are 1.02 and 1.04, respectively. As shown in the inset of Fig. 7, the output laser beam closely resembled the standard Gauss distribution, which benefitted from the favorable astigmatism compensation by optimizing the cavity structure. Lastly, the tuning characteristics of the Ti:S laser are tested by a wavelength meter (WS6/765, High Finesse) under SLM operation. The output powers of the Ti:S laser at different output wavelengths are illustrated in Fig. 8. It is obvious that the wavelength of the output laser is tuned

Optics EXPRESS

from 760 nm to 882 nm by rotating the BRF, and the maximal tuning range of 122 nm is achieved. This tuning range is restricted by the coated films of cavity mirrors and the designed BRF with a broad tuning range. The maximum output power at 786 nm reaches 3 W when the incident pump power is 12 W. At this time, it seems that the output power is about 2.47 W when the wavelength of the Ti:S laser is 824 nm. When the etalon is locked to the oscillating longitudinal-mode of the Ti:S laser near the wavelength of 824 nm, by changing the voltage loaded on the PZT to scan the length of the laser cavity, the continuous frequency-tuning range of 24 GHz is realized, which is shown in Fig. 9.

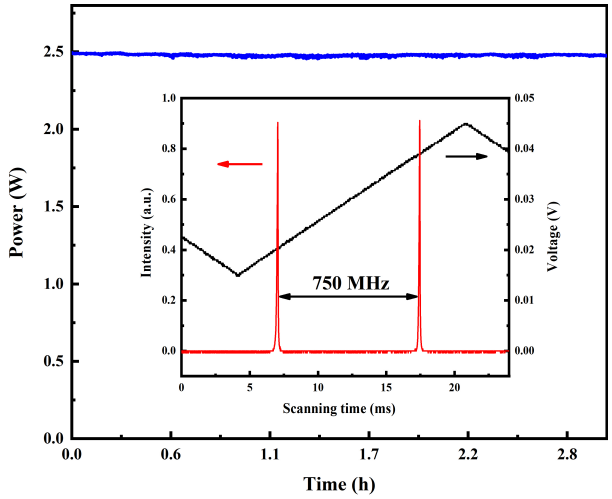

Fig. 6. Measured long-term power stability of the output laser over 3 hours. Inset shows the longitudinal-mode structure of the Ti:S laser

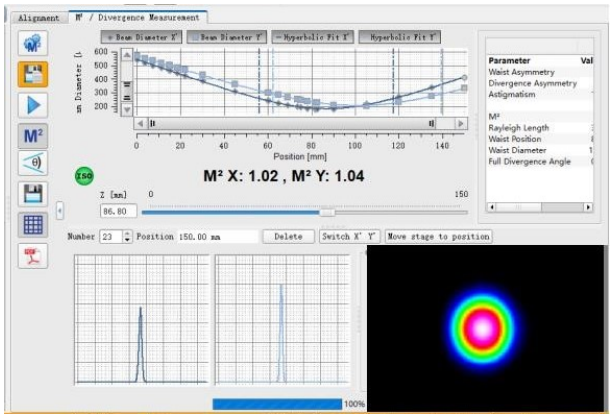

Fig. 7. Measured M^2 values and spatial beam profile of the Ti:S laser.

Optics EXPRESS

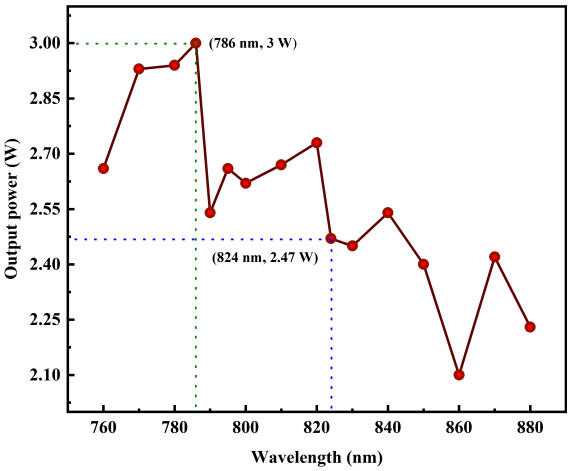

Fig. 8. Output power of the Ti:S laser as a function of the operating wavelength.

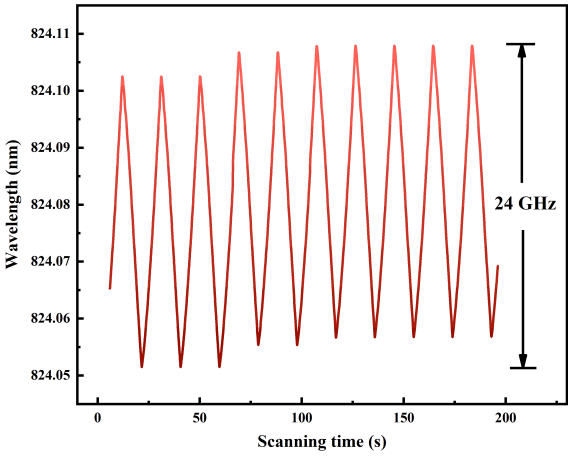

Fig. 9. Continuous frequency-tuning range of the Ti:S laser.

4. Conclusions

In summary, in this paper we present a novel single-frequency tunable Ti:S laser which is immune to the noise of the pump source. Both the theoretical predictions and experimental results demonstrate that the intensity noise of the pump source in the low frequency band is easily transferred to the built Ti:S laser. Because this frequency band happens to cover that of the modulation signals for the IE locking, the intensity noise of the pump source can directly disturb the IE locking stability. However, when the common detector is replaced by a differential detector with dual-PDs, this influence on the error signal for IE locking is easily eliminated since the intensity noise of the Ti:S laser detected by PD2 is subtracted by that of the pump source detected by PD1. The experimental results well agree to the theoretical predictions. At last, an all-solid-state CW single-frequency tunable Ti:S laser with immunity to the intensity noise of the pump source is attained. By recording its long-term power fluctuation and measuring the beam quality, it is seen that the high power stability better than ±0.8% for 3 hours and beam quality better than 1.1 are obtained, which further reveals the importance of the differential

Optics EXPRESS

detector for the IE locking. The developed method is suitable for lasers where the IE can not be stably locked due to the large noise of the pump sources and paves a good way to realize a stable single-longitudinal-mode laser or a continuous tunable laser with the mode-hop-free by adopting IE locking systems.

Funding. National Natural Science Foundation of China (61975100, 62027821, 62105192); Applied Basic Research Project of Shanxi Province, China (20210302121004); Key R&D Program of Shanxi Province (202102150101002); Program for the Innovative Talents of High Education Institutions of Shanxi; Fund for Shanxi "1331 Project" Key Subjects Construction; Research Project Supported by Shanxi Scholarship Council of China (2022-015).

Disclosures. The authors declare no conflicts of interest.

Data availability. Data underlying the results presented in this paper are not publicly available at this time but may be obtained from the authors upon reasonable request.

References

1. W. Vassen, C. Zimmermann, R. Kallenbach, and T. W. Hänsch, "A frequency-stabilized titanium sapphire laser for high-resolution spectroscopy," Opt. Commun. **75**(5-6), 435–440 (1990).
2. H. J. Kimble, "The quantum internet," Nature **453**(7198), 1023–1030 (2008).
3. B.-B. Li, J. Bílek, U. B. Hoff, L. S. Madsen, S. Forstner, V. Prakash, C. Schäfermeier, T. Gehring, W. P. Bowen, and U. L. Andersen, "Quantum enhanced optomechanical magnetometry," Optica **5**(7), 850–856 (2018).
4. Y. Wei, H. Lu, P. Jin, and K. Peng, "Self-injection locked CW single-frequency tunable Ti:sapphire laser," Opt. Express **25**(18), 21379–21387 (2017).
5. J. Wei, X. Cao, P. Jin, Z. Shi, J. Su, and H. Lu, "Realization of compact Watt-level single-frequency continuous-wave self-tuning titanium: sapphire laser," Opt. Express **29**(2), 2679–2689 (2021).
6. T. Kuwamoto, K. Honda, Y. Takahashi, and T. Yabuzaki, "Magneto-optical trapping of Yb atoms using an intercombination transition," Phys. Rev. A **60**(2), R745–R748 (1999).
7. P. Fan, Y. Li, S. Li, J. Yuan, and L. Wang, "Experimental investigation on the 420 nm blue light generated by two-photon transition of Rb," J. Quantum Opt. **23**(2), 144–150 (2017).
8. R. Ma, W. Liu, Z. Qin, and F. Li, "Realization of optical phase-locked loop and its application in four-wave mixing process in cesium vapor," J. Quantum Opt. **24**(3), 343–348 (2018).
9. K. I. Martin, W. A. Clarkson, and D. C. Hanna, "Self-suppression of axial mode hopping by intracavity second-harmonic generation," Opt. Lett. **22**(6), 375–377 (1997).
10. H. Lu, X. Sun, M. Wang, J. Su, and K. Peng, "Single frequency Ti:sapphire laser with continuous frequency-tuning and low intensity noise by means of the additional intracavity nonlinear loss," Opt. Express **22**(20), 24551–24558 (2014).
11. P. Jin, H. Lu, Q. Yin, J. Su, and K. Peng, "Expanding continuous tuning range of a CW single-frequency laser by combining an intracavity etalon with a nonlinear loss," IEEE J. Sel. Top. Quantum Electron. **24**(5), 1–5 (2018).
12. X. Yang, O. Kitzler, D. J. Spence, Z. Bai, Y. Feng, and R. P. Mildren, "Diamond sodium guide star laser," Opt. Lett. **45**(7), 1898–1901 (2020).
13. X. Yang, Z. Bai, D. Chen, W. Chen, Y. Feng, and R. P. Mildren, "Widely-tunable single-frequency diamond Raman laser," Opt. Express **29**(18), 29449–29457 (2021).
14. J. Harrison, A. Finch, J. H. Flint, and P. F. Moulton, "Broad-band rapid tuning of a single-frequency diode-pumped neodymium laser," IEEE J. Quantum Electron. **28**(4), 1123–1130 (1992).
15. S. Kobtsev, V. Baraoulya, and V. Lunin, "Ultra-narrow-linewidth combined CW Ti:sapphire/dye laser for atom cooling and high-precision spectroscopy," Proc. SPIE **6451**, 64511U (2007).
16. X. Sun, J. Wei, W. Wang, and H. Lu, "Realization of a continuous frequency-tuning Ti:sapphire laser with an intracavity locked etalon," Chin. Opt. Lett. **13**(7), 071401 (2015).
17. P. Jin, H. Lu, Y. Wei, J. Su, and K. Peng, "Single-frequency CW Ti:sapphire laser with intensity noise manipulation and continuous frequency-tuning," Opt. Lett. **42**(1), 143–146 (2017).
18. K. S. Gardner, R. H. Abram, and E. Riis, "A birefringent etalon as single-mode selector in a laser cavity," Opt. Express **12**(11), 2365–2370 (2004).
19. P. Jin, Y. Xie, X. Cao, J. Su, H. Lu, and K. Peng, "Modulation-noise-free continuously tunable single-frequency CW Ti:Sapphire laser with intracavity-locked birefringent etalon," IEEE J. Quantum Electron. **58**(1), 1–6 (2021).
20. S. M. Kobtsev, V. I. Baraulya, and V. M. Lunin, "Combined cw single-frequency ring dye/Ti:sapphire laser," Quantum Electron. **36**(12), 1148–1152 (2006).
21. H. Lu, J. Su, C. Xie, and K. Peng, "Experimental investigation about influences of longitudinal-mode structure of pumping source on a Ti:sapphire laser," Opt. Express **19**(2), 1344–1353 (2011).
22. Y. Sun, H. Lu, and J. Su, "Continuous-wave, single-frequency, all-solid-state Ti:Al_2O_3 laser," J. Quantum Opt. **52**(3), 344–347 (2008).